

RSC Advances



This is an *Accepted Manuscript*, which has been through the Royal Society of Chemistry peer review process and has been accepted for publication.

Accepted Manuscripts are published online shortly after acceptance, before technical editing, formatting and proof reading. Using this free service, authors can make their results available to the community, in citable form, before we publish the edited article. This *Accepted Manuscript* will be replaced by the edited, formatted and paginated article as soon as this is available.

You can find more information about *Accepted Manuscripts* in the [Information for Authors](#).

Please note that technical editing may introduce minor changes to the text and/or graphics, which may alter content. The journal's standard [Terms & Conditions](#) and the [Ethical guidelines](#) still apply. In no event shall the Royal Society of Chemistry be held responsible for any errors or omissions in this *Accepted Manuscript* or any consequences arising from the use of any information it contains.

ARTICLE

Polarization-selective polymerization in a photo-crosslinking monomer film

Cite this: DOI: 10.1039/x0xx00000x

My-Phung Van,^a Carl C.L. Schuurmans,^a Cees W.M. Bastiaansen^{a,b} and Dirk J. Broer^{a,c}Received 00th January 2014,
Accepted 00th January 2014

DOI: 10.1039/x0xx00000x

www.rsc.org/

The molecular order in a smectic monomer is utilized to create a photoreactive material that is highly polarization-selective during its photo-crosslinking polymerization. A dichroic photoinitiator adapts the molecular orientation of its aligned smectic B host monomer which reaches a degree of orientation larger than 0.9. This value correlates to a dichroic ratio, defined as the absorbance ratio of light with its polarization respectively parallel and perpendicular to the orientation axis, of 32. This is substantially higher than the dichroic ratio of similar dichroic initiators previously studied in nematic host monomers which considerably improves the polymerization contrast. The presence of an inhibitor, such as a hydroquinone, in the monomeric mixture enhances the polymerization contrast further. The effect of the inhibitor is due to the close to zero monomer to polymer conversion for the polarization perpendicular to the alignment in the initial stages of polymerization. It is argued that the high polarization-selectivity of the above-described system is potentially useful in nano and/or microstructuring techniques without the use of masks such as polarization holography.

1. Introduction

Optical lithography is nowadays widely used to generate patterned structures with dimensions in the nano and micrometer range.¹⁻⁴ Typically, a negative or positive photoresist is exposed to a light intensity pattern using a mask and, dependent on the type of photoresist, the illuminated or non-illuminated regions are developed to reproduce the pattern of the mask. Almost exclusively, isotropic photoresists^{1, 5-7} are employed and an enormous range of structures, components and devices is produced.

Anisotropic photoresist materials with a well-defined monodomain alignment have also been explored in lithographic applications.^{8, 9} In most cases, negative photoresist materials were used based on reactive liquid crystalline (LC) monomers containing a dichroic photoinitiator. These rod-shaped initiators are capable to adapt to the molecular alignment of the LC monomer host. The transition moment along the long molecular axis of the photoinitiator aligns with the monomer orientation (director) making it selective for absorption of light with its electrical field vector parallel to the orientation and relatively insensitive for light with the orthogonal polarization. The polarization-selectivity can be characterized by the dichroic ratio (DR), which is defined as the ratio of the absorbed light parallel (A_{\parallel}) and perpendicular (A_{\perp}) to the director (Eq. 1). This

number ranges from unity for an isotropic system to infinity for a perfectly uni-axially aligned system.

In literature a dichroic photoinitiator is used in combination with nematic LC mesogens with a planar, splay or chiral-nematic alignment. The alignment is controlled by alignment layers coated on the substrate often in combination with chiral dopants or planarization additives.¹⁰ The polarization-selectivity enabled patterning using the dependence of monomer to polymer conversion on the polarization state of light and the local molecular director. Both mask and maskless exposures were used leading to a variety of structures, some of them not one-to-one possible by using traditional lithography. In these studies, nematic host materials were used which exhibit a rather low order parameter of between 0.6 and 0.7 and, hence, resulted in poorly defined microstructures.⁹

$$DR = \frac{A_{\parallel}}{A_{\perp}} \quad \text{Eq. 1}$$

An enhanced polarization-selectivity is desired in order to create well-defined patterns. One way of achieving the higher ratio is to use the more ordered smectic B (SmB) liquid crystalline phase as is for instance shown for the dichroic absorption of dye molecules in polarizer films.¹¹ In this paper we demonstrate the polarization-selectivity of the photopolymerization of a SmB acrylate monomer. We also

study further enhancement of this polarization-selective polymerization by adding free-radical scavengers which makes the response of the resist towards light highly non-linear by consuming initial radical initiators. This non-linear effect is a desired property for lithographic formulations.¹²⁻¹⁴

2. Experimental

The photoreactive mixture consists of the materials shown in Fig. 1. Dichroic photoinitiator **1** (1 wt%) was supplied by Merck. The LC host comprises of monoacrylate **2**¹¹ and crosslinker **3**.¹⁵ Inhibitor 4-methoxyphenol **4** (0.5 wt%) was supplied by Sigma-Aldrich.

The thermal behavior of the reactive mixture was characterized with differential scanning calorimetry (DSC) TA Instrument Q1000 calorimeter. 1-2 mg was weighed in a hermetically sealed aluminum pan. The LC mixture was heated from 20 °C to 160 °C and then cooled back to 20 °C at a heating and cooling rate of 10 °C min⁻¹.

Polarized optical microscopy (POM) was performed with a Leica CTR 6000 microscope equipped with crossed polarizers to examine the phase behavior. For this analysis the LC mixture was sandwiched between two glass slides (cell) coated with polyimide (PI) JSR Micro AL-24101. The polyimide alignment layer was spincoated on the glass substrates with a two-step program: 1000 rpm for 5 s and subsequently 5000 rpm for 30 s. In both steps the acceleration was 2000 rpm s⁻¹. After spincoating, the substrates were placed on a hotplate at 85 °C for 1 min before being baked for 90 min in an oven set at 180 °C. In order to observe textures to characterize the LC phases, defects were introduced to the polyimide surfaces by a razorblade. The material was heated and cooled down in a Linkam hot-stage THMS600 and images were recorded, upon cooling, with a Leica DFC420 C camera.

Small and wide angle x-ray scattering (SAXS/WAXS) were performed on samples sealed in a 1 mm glass capillary inside a custom-built heating stage equipped with a 1 T permanent magnetic field. The material was heated with a rate of 30 °C min⁻¹ to the isotropic phase first before being cooled down with 10 °C min⁻¹. The monomer mixtures were analyzed upon cooling. The samples were irradiated with a 1.54 Å GeniX-Cu ultra-low divergence source. The diffraction patterns were recorded on a Pilatus 300K silicon pixel detector. Silver behenate was used for calibration.¹⁶ The order parameter of the aligned material was calculated based on Eq. 2,¹⁷ where θ is the azimuthal angle as defined in Fig. 3-P3.

$$S = \frac{\int_{-1/2\pi}^{1/2\pi} I(\theta) \frac{3\cos^2\theta - 1}{2} \sin\theta d\theta}{-\frac{1}{2} \int_{-1/2\pi}^{1/2\pi} I(\theta) \sin\theta d\theta} \quad \text{Eq. 2}$$

The absorbance spectra of the dichroic photoinitiators in the aligned LC host were recorded on a Shimadzu UV-3102 spectrophotometer equipped with a wire grid polarizer

(PPL05A Moxtek). 2-4 μm thick films were prepared in a cell by using glass spacers. Uni-axial alignment was achieved by coating the glass plates with anti-parallel rubbed polyimide (JSR Micro AL-2410). Rubbing was done manually with a cloth. The cells were filled through capillary action at 140 °C and cooled down to room temperature for the measurement.

The conversion of the C=C acrylate bonds was monitored using Fourier Transform Infrared spectroscopy (FTIR) on a Varian 610-IR spectrometer that was equipped with a microscope. The spectra were recorded in reflection mode with a resolution of 2 cm⁻¹. For this purpose thin 2-4 μm films were prepared in a cell. In order to be able to measure in reflection mode a cell was made comprising of a glass plate coated with gold and rubbed polyimide, as described previously, and a CaF₂ infrared transparent window coated with rubbed polyimide. The photoreactive material was exposed with an EXFO Omnicure Series 2000 mercury lamp (2.1 mW cm⁻²). The measurements were carried out in both N₂ atmosphere and in air. The degree of conversion is defined as the percentage of moles of C=C acrylate bonds (1408 cm⁻¹) converted. All spectra were normalized with the aromatic C=C signal (1511 cm⁻¹).

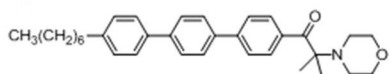
Dose-response curves were obtained by illuminating the LC material with different exposure times with an EXFO Omnicure Series 2000 mercury lamp. The material was aligned uni-axially in a cell where one glass substrate was coated with polyimide (JSR Micro AL-24101) and the other glass substrate was coated with polyvinyl alcohol (PVA). Two different alignment layers were used to have the formed polymer layer remaining on a single substrate after opening the cell. The polymerized LC material adheres better to PVA than PI. A 5 wt% aqueous PVA solution was spin coated on the glass at 2000 rpm for 30 s and with an acceleration of 500 rpm s⁻¹. Subsequently, the substrate was baked for 30 min at 90 °C. Both alignment layers were rubbed with a cloth after which the cell was fabricated. Before filling the cell with the reactive mixture, the cell gap was measured by wavelength-dependent interference using a spectrophotometer (Shimadzu UV-3102).¹⁸ After filling the cell at 140 °C through capillary action, the reactive mixture in the cell was exposed at RT with linearly polarized light with a specific dose and subsequently the cell was opened. The material was developed with acetone for 5-10 s. The remaining film thickness was measured using a 3D interferometer (Fogal Nanotech Zoomsurf). The response R is defined as the remaining film thickness d normalized with the cell gap d^0 ($R = d/d^0$). The response is plotted as a function of the dose D (mJ cm⁻²) which is the product of the intensity I of the UV-illumination (2.1 mW cm⁻²) and the time t of exposure ($D = I \cdot t$)

3. Results & Discussion

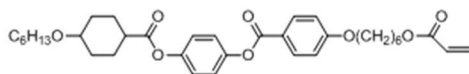
The LC host material used to align the dichroic photoinitiator is monomer **2**¹¹ (Fig. 1) which upon melting at 45 °C shows liquid crystalline behavior. Heated above 147 °C the monomer is isotropic. In the liquid crystalline state it has been previously shown that this material exhibits a nematic phase between

112 °C and 147 °C and additionally there are two smectic phases upon further cooling, namely smectic A (SmA) between 56 °C and 112 °C and smectic B (SmB) below 56 °C. For the smectic phases it is well known that they exhibit a higher degree of order compared to the more often observed nematic phase in liquid crystalline monomers.^{11, 19, 20} Since the polarization-selectivity of the dichroic photoinitiator largely depends on the order of the host, it is expected that in the SmB phase, which exhibits the highest degree of order, a higher polarization-selectivity can be achieved. LC host **2** is a monoacrylate which forms a linear polymer upon polymerization. In order to form a better solvent-resistant polymer network, a di-functional crosslinker **3** is mixed with **2** (20/1 wt/wt ratio of **2** and **3**). Crosslinker **3** was selected based on the similarity of the molecular structure with host **2** to prevent disruption of the desired highly ordered smectic phases of **2**. The crosslinker itself is known to exhibit a nematic phase and a smectic C phase in a supercooled state.¹⁵ Hydroquinone based materials are commonly used as inhibitor but are also known to enhance the contrast in acrylate based lithographic materials.¹²⁻¹⁴ Therefore, inhibitor **4** (0.5 wt%) is added to the system to increase the polarization-selectivity of the photopolymerization.

Dichroic photoinitiator **1**:

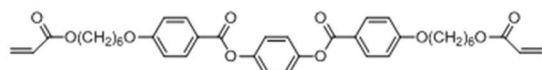


Liquid crystal host **2**:



Cr 45 °C SmB 56 °C SmA 112 °C N 147 °C I

Crosslinker **3**:



(SmC 89 °C) Cr 108 °C N 153 °C I

Inhibitor **4**:

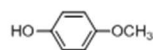


Fig. 1 Molecular structures of the dichroic photoinitiator, smectic B LC host¹¹, crosslinker¹⁵ and inhibitor

Due to the presence of the smectic B phase in monomer **2**, this material was selected. However, the addition of compounds **1**, **3** and **4** might affect the phase behavior of monomer **2**. Therefore, the phase behavior of the full mixture with four compounds as described above is characterized. The phase transition temperatures of this mixture were determined by DSC (Fig. 2). Upon heating, the mixture shows mesomorphic phase transitions at 54 °C and 108 °C; and above 145 °C the material becomes isotropic (Fig. 2, P1). Upon cooling, the mixture shows the same transition temperatures and remains liquid

crystalline at room temperature for approximately two hours before crystallization occurs. The supercooled state enables processing of the mixture at room temperature. The LC phases exhibit thread-like textures (Fig. 2-P2) and fan-shaped textures (Fig. 2-P3 and P4) which are characteristic for the nematic and smectic phases, respectively.²⁰ To identify the LC phases, the photoreactive mixture was further characterized with x-ray diffraction.²¹

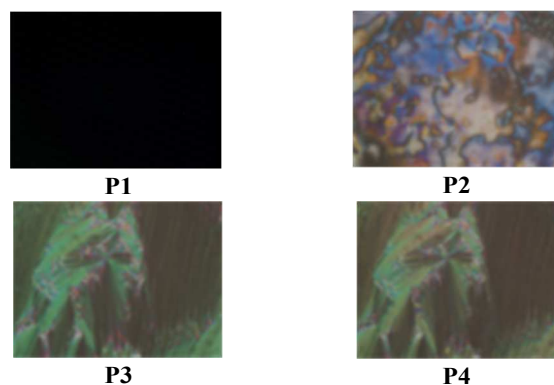
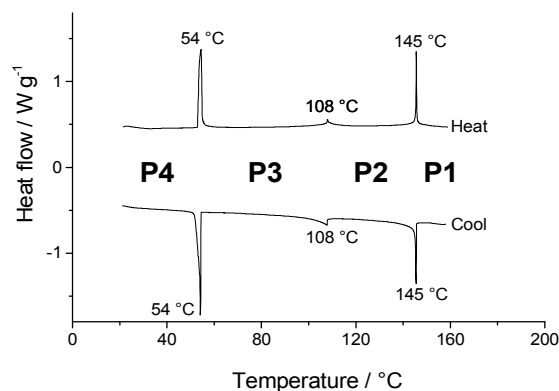


Fig. 2 The DSC curve of the second heating and cooling cycle of the photoreactive mixture and the corresponding optical microscopy images between crossed polarizers of the phases P1-P4 obtained upon cooling of the material.

The diffraction patterns for the three different phases are shown in Fig. 3. In every phase two sets of diffraction patterns appear, namely a SAXS signal corresponding to the periodicity of the smectic layers (d_L) and a WAXS signal corresponding to the intermolecular distance (d_I).²¹ The unexpected appearance of a SAXS signal in P2 (Fig. 3-P2), the presumed simple nematic phase, indicates the formation of local layer-like domains. This phase is known as the cybotactic nematic phase (N_C); thus, confirming the cybotactic nematic phase between 108 °C and 145 °C. The appearance of the SAXS signal in the smectic phases P3 and P4 are expected (Fig. 3-P3 and P4). More diffraction orders are visible for P4 compared to P3, explained by the higher degree of order of P4. The WAXS signal of P4 is also more intense compared to P3. Based on this result, P3 and P4 are the LC phases smectic A and B, respectively. In the SmB phase, the molecules are hexagonally packed and,

therefore, are more ordered compared to SmA. Based on the DSC, POM and SAXS/WAXS analyses, the liquid crystalline phase behavior of the photoreactive mixture is: SmB 54 °C SmA 108 °C N_c 145 °C I. Aside from minor changes in transition temperatures, the type of phases of LC monomer **2** remains unaffected by the addition of dichroic photoinitiator **1**, crosslinker **3** and inhibitor **4**.

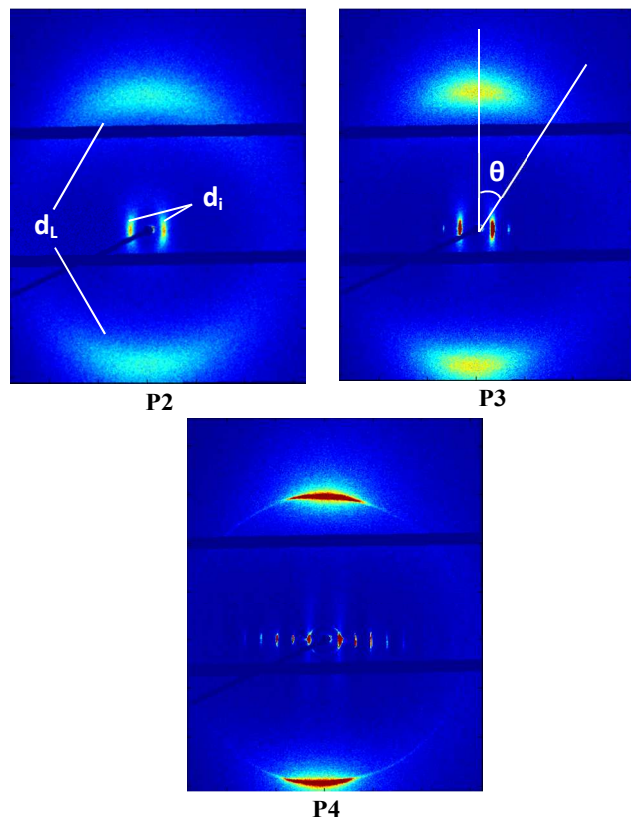


Fig. 3 The diffraction patterns of phases P2, P3 and P4. The SAXS signal arises from the smectic layers (d_L). The WAXS signal arises due to the intermolecular distance (d_i). θ is the azimuthal angle.

The periodicity and the intermolecular distance of the smectic layers are shown in Table 1. The d_L value increases, going from N_c to SmA and to SmB. With increasing order, the molecules have a lower average tilt from the director, resulting in a layer spacing which corresponds closest to the length of the molecule of host **2** in the SmB phase. d_i decreases for increasingly ordered phases, indicating a more densely packed LC phase. Based on the WAXS signal an order parameter can be calculated according to Eq. 2. The order parameter is 0.70 ± 0.05 , 0.82 ± 0.03 and 0.94 ± 0.01 for N_c, SmA and SmB, respectively. Assuming that the dichroic photoinitiator adopts the order of its LC host and that the transition moment is perfectly parallel to the long axis of initiator, a dichroic ratio (DR) of 8, 15 and 48 is deduced for the respective phases.²²

Table 1 The values for the periodicity of the smectic layers (d_L) and intermolecular distance (d_i) for the three LC phases.

	$d_L / \text{Å}$	$d_i / \text{Å}$
N _c	35.2	4.62
SmA	37.8	4.58
SmB	39.7	4.47

The high dichroic ratio of the host, determined with WAXS, is only advantageous if dichroic photoinitiator **1** indeed aligns with the LC host. To examine the alignment of **1**, polarization-dependent absorbance spectra were measured for a uni-axially aligned monomer mixture containing the dichroic photoinitiator (Fig. 4). The wavelength of maximum absorbance shifts to below 325 nm going from SmB to SmA and N_c phase. A possible explanation is the change of molecular packing of the host molecules in the different LC phases that affect the electronic transition of the dichroic photoinitiator. An additional comment should be made regarding the shape of the absorbance spectra of the SmB phase parallel and perpendicular to the molecular director which is not identical. This asymmetry could be caused by an intensification of higher energy electronic vibrations perpendicular to the long axis of the photoinitiator molecule. A definitive explanation requires further investigation which falls outside the scope of this study. An important conclusion is that all phases show polarization-selectivity due to the added photoinitiator. A dichroic ratio of 5, 10 and 32 at 355 nm is measured for the N_c, SmA and SmB phase, respectively. These numbers correspond to order parameters of 0.40 ± 0.1 , 0.75 ± 0.05 and 0.91 ± 0.01 for the photoinitiator in the respective phases. For both the application of magnetic field as well as alignment layers a monodomain is formed. Therefore, it is assumed that the order parameter of the LC monomeric host mixture is the same for both alignment techniques. The dichroic ratios measured here are lower compared to the value calculated from WAXS. This difference might be due to an angle between the transition moment of initiator **1** and the long molecular axis of the molecule and/or the fact that **1** does not align perfectly with the host. It should also be stated that the values for high dichroic ratios are very sensitive to the baseline correction of the spectra which further complicates the accurate measurement of the dichroic ratios. These ratios determined via the absorbance spectra do confirm that the host largely determines the alignment of the dichroic photoinitiator and, additionally, this result also shows polarization-selectivity of the photoreactive mixture in all the LC phases. The highest dichroic ratio in SmB validates that the highest polarization-selectivity can be achieved in this phase.

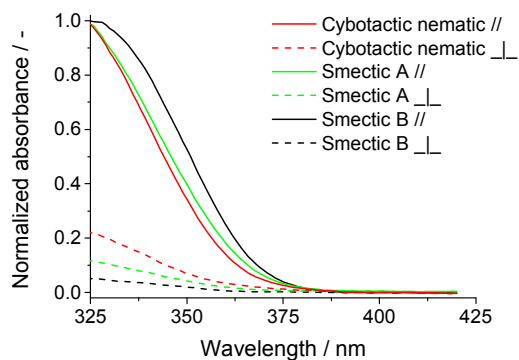


Fig. 4 Absorbance spectra of the dichroic photoinitiator **1** aligned in the monomer mixture of **2** and **3** for linearly polarized light parallel (//) and perpendicular (\perp) to the director. Only partial absorption spectra are shown due to the absorption of the LC host **2** below 325 nm.

The difference in absorbance parallel and perpendicular to the director results in a difference in polymerization rate (R). Previously it was shown that the polymerization contrast ($R_{//}/R_{\perp}$) scales with the square root of the dichroic ratio (Eq. 3).²³

$$\frac{R_{//}}{R_{\perp}} \propto \sqrt{\frac{A_{//}}{A_{\perp}}} \quad \text{Eq. 3}$$

$R_{//}$ is the polymerization rate with the polarization parallel to the director and R_{\perp} is the rate with the polarization orthogonal to the director. This relation is only valid in the initial polymerization stage where mobility limitations do not affect the polymerization kinetics and termination predominantly occurs via a bi-molecular process.^{24, 25} Here we measured the polymerization contrast of the uni-axially aligned material in the SmB phase by monitoring the C=C acrylate bond conversion as a function of time. Measurements were done both in nitrogen atmosphere and in air (Fig. 5); and always in the presence of inhibitor **4**. A film of the photoreactive mixture with controlled thickness was prepared via capillary action between two spaced glass plates (cell) at elevated temperatures. Inhibitor **4** functions to prevent thermal polymerization as well as to increase the polymerization contrast. The initial polymerization rate is defined as the tangent of the conversion-time curve at the onset of polymerization directly after the inhibition period. A clear difference in polymerization rate between the parallel and perpendicular configuration is observed in both nitrogen atmosphere and in air. The contrast in polymerization rate can be assigned to the difference in absorption by the photoinitiator for the two illumination configurations.

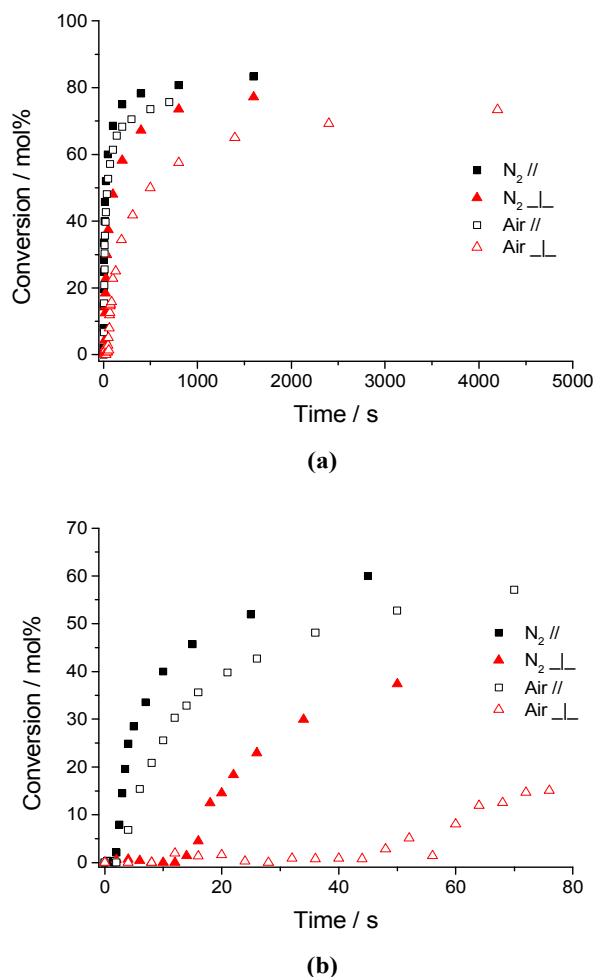


Fig. 5 a) Conversion as function of time and b) a magnification of the initial polymerization stage. The curves were obtained in the smectic B phase at RT.

In nitrogen atmosphere, the observed inhibition period is assumed to be caused by the presence of inhibitor **4**. These inhibitor molecules largely retard polymerization until they have all reacted with the first free initiator radicals formed. After the inhibition period, the polymerization rates of the reaction are $12.1 \text{ mol\% s}^{-1}$ for parallel illumination and 2.3 mol\% s^{-1} for perpendicular illumination, which results in a polymerization contrast of 5.3, which roughly corresponds to the value of 5.7 (square-root of 32) based on Eq. 3. This value for the SmB phase is higher compared to a value of 2.6 for the nematic phase obtained in a previous study where the polymerization was also performed in a nitrogen environment with another nematic host and dichroic photoinitiator.²³ This confirms our assumption that by enhancing uni-axial alignment of the dichroic photoinitiator in the SmB host, the polymerization contrast and, therefore, polarization-selectivity is improved.

In the presence of oxygen, the polymerization rates at the onset of the reaction are 3.8 mol\% s^{-1} and 0.5 mol\% s^{-1} for parallel and perpendicular illumination, respectively. This leads to a

polymerization contrast of 7.6. The lower polymerization rates are explained by an enhanced inhibition due to the synergy between inhibitor 4 and oxygen.²⁵ Oxygen itself is known to be an affective inhibitor, but oxygen is also known to increase the activity of phenol inhibitors. Therefore, the inhibition period is also longer compared to polymerization performed under nitrogen. A comment should be made regarding the difference in inhibition time between parallel and perpendicular illumination for the nematic and smectic B phase. Though no results for the nematic phase are shown here, it is probable that the difference in inhibition time for the two illumination configurations is larger in the SmB phase due to the higher dichroic ratio in this phase. During the inhibition period, in the presence of inhibitor with and without oxygen, there is a period where the LC mixture is only sensitive to parallel illumination (Fig. 5). Under nitrogen at the end of the perpendicular inhibition period, a condition can be reached where the conversion for parallel illumination is 40 mol% while the conversion for perpendicular illumination is 0 mol%. In the presence of oxygen the conversion is 50 mol% and 0 mol%, respectively, i.e. the contrast under these conditions is practically infinite and the difference in conversion can be tuned by controlling the amount of inhibitor and/or the controlled addition of oxygen.

As stated, an important use of the polarization-selectivity is polarization-selective lithography. For lithographic purposes, the so-called dose-response curve is relevant. This curve provides information on the relative thickness of the polymerized pattern that remains after a development step during which unreacted monomers are dissolved. Fig. 6 shows the dose-response curve for two polarization directions of light with respect to the director. Up to a dose of 30 mJ cm⁻², only structures remain after solvent development when exposed with the polarization of the UV illumination parallel to the director. Under similar conditions, the substrate remains clean when exposed with orthogonal polarization which is a favorable condition for lithographic purposes. This result shows that the illumination dose should not exceed 30 mJ cm⁻² to maintain the high polarization-selectivity of the material. With this dose the response is 0.6. To increase the response (or conversion) a post-exposure bake should be applied to form well-defined polymer patterns as desired in lithographic processes. The high polarization-selectivity of the photoreactive mixture developed here can be used for pattern formation in maskless lithography such as polarization holography which is under investigation.

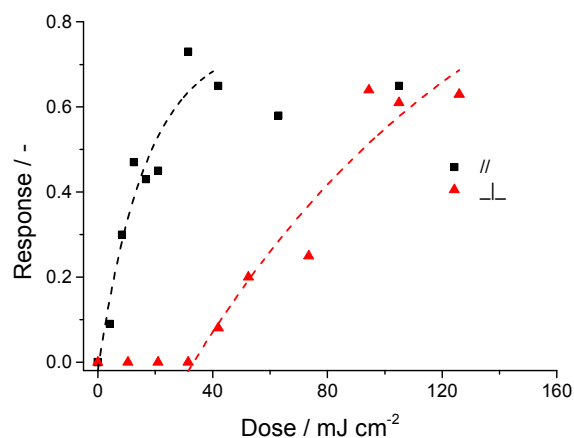


Fig. 6 The initial stage of the dose-response curve of the smectic B photoreactive material in nitrogen atmosphere.

4. Conclusions

We have shown that a photopolymerizable composite with high polarization-selectivity can be created by adding a dichroic photoinitiator to a reactive smectic B host and aligning this material uni-axially on a pre-treated surface. We have shown that the polymerization-contrast is increased from 2.6 to 7.6 by performing the polymerization in the presence of inhibiting species and using a well-ordered SmB host instead of the nematic phase used in previous studies.^{9,23} In combination with an inhibitor in the reactive monomer mixture the polarization-selectivity is shown to be infinite. The dose-response was measured, and it is shown that a high polarization-selectivity is obtained which potentially can be useful for lithographic purposes without mask, such as polarization holography.

Acknowledgements

The authors acknowledge the support of the Stichting voor Technische Wetenschappen (STW project 10727). Additionally, we acknowledge Merck for supplying the dichroic photoinitiator; and the Institute for Complex Molecular Systems and Berry Bögels for making it possible to perform the SAXS and WAXS measurements.

Notes and references

^a M.P. Van MSc, C.C.L. Schuurmans, Prof D.J. Broer
Functional organic Materials & Devices

Department of Chemical Engineering and Chemistry
Eindhoven University of Technology
5600 MB Eindhoven, The Netherlands
E-mail: D.Broer@tue.nl

^b Prof C.W.M. Bastiaansen
School of engineering and materials science
Queen Mary, University of London
London E1 4NS, United Kingdom
Email: c.w.m.bastiaansen@qmul.ac.uk

© Prof. D.J. Broer

Institute for Complex Molecular Systems

Eindhoven University of Technology

5600 MB Eindhoven, The Netherlands

E-mail: D.Broer@tue.nl

1. K. Suzuki and B. W. Smith, *Microlithography*, Taylor & Francis Group, LLC, Boca Raton, 2007.
2. T. Ito and S. Okazaki, *Nature*, 2000, **406**, 1027.
3. R. P. Seisyan, *Tech. Phys.*, 2011, **56**, 1061-1073.
4. G. M. Wallraff and W. D. Hinsberg, *Chem. Rev.*, 1999, **99**, 1801-1821.
5. H. Ito, in *Microlithography - Molecular Imprinting*, Springer-Verlag Berlin, Berlin, 2005, pp. 37-245.
6. H. Ito, *J. Photopolym. Sci. Technol.*, 2008, **21**, 475-491.
7. H. Tsubaki, S. Tarutani, N. Inoue, H. Takizawa and T. Goto, *J. Photopolym. Sci. Technol.*, 2013, **26**, 649-657.
8. D. J. Broer, G. N. Mol, J. A. M. M. v. Haaren and J. Lub, *Adv. Mater.*, 1999, **11**, 573-578.
9. B. Serrano-Ramon, C. Kjellander, S. Zakerhamidi, C. W. M. Bastiaansen and D. J. Broer, in *Emerging Liquid Crystal Technologies III*, Spie-Int Soc Optical Engineering, Bellingham, 2008, pp. 1-13.
10. K. Takatoh, M. Hasegawa, M. Koden, N. Itoh, R. Hasegawa and M. Sakamoto, *Alignment technologies and applications of liquid crystal devices*, Taylor & Francis group, LLC, 2005.
11. E. Peeters, J. Lub, J. A. M. Steenbakkers and D. J. Broer, *Adv. Mater.*, 2006, **18**, 2412-2417.
12. S. Kawata, H. B. Sun, T. Tanaka and K. Takada, *Nature*, 2001, **412**, 697-698.
13. T. F. Scott, B. A. Kowalski, A. C. Sullivan, C. N. Bowman and R. McLeod, *Science*, 2009, **324**, 913-917.
14. Y. Cao, Z. Gan, B. Jia, R. A. Evans and M. Gu, *Opt. Express*, 2011, **19**, 19486-19494.
15. D. J. Broer, in *Radiation curing in polymer science and technology*, eds. J. P. Fouassier and J. F. Rabek, Elsevier applied science, 1993.
16. K. Binnemans, R. Van Deun, B. Thijs, I. Vanwelkenhuysen and I. Geuens, *Chem. Mat.*, 2004, **16**, 2021-2027.
17. G. R. Mitchell and R. Lovell, *Acta Crystallogr. Sect. A*, 1981, **37**, 189-196.
18. K. H. Yang, *J. Appl. Phys.*, 1988, **64**, 4780-4781.
19. A. J. Leadbetter and P. G. Wrighton, *J. Physique*, 1979, **40**, C3-234 - C233-242.
20. I. Dierking, *Textures of liquid crystals*, Wiley-VCH Verlag GmbH & Co. KGaA, Weinheim, 2003.
21. D. Demus, J. Goodby, G. W. Gray, H.-W. Spiess and W. Vill, *Volume 1: Fundamentals*, Wiley-VCH verlag GmbH, Weinheim, 1998.
22. B. E. Read and R. S. Stein, *Macromolecules*, 1968, **1**, 116-126.
23. D. J. Broer, *Curr. Opin. Solid State Mater. Sci.*, 2002, **6**, 553-561.
24. M. G. Joshi, *Journal of Applied Polymer Science*, 1981, **26**, 3945-3946.
25. G. Odian, *Principles of polymerization*, Wiley-interscience, Hoboken, New Jersey, 2004.